

Improved prestressed concrete girder with hybrid segments system

Hong Jae Yim^{1a}, Jun Mo Yang^{2b} and Jin Kook Kim^{*2}

¹Department of Construction and Disaster Prevention Engineering, Kyungpook National University, 2559 Gyeongsang-daero, Sangju, Gyeongsangbuk-do, 742-711, Republic of Korea

²Product Application Center, POSCO, 100, Songdowahak-ro, Yeonsu-gu, Incheon, 406-840, Republic of Korea

(Received December 15, 2017, Revised December 17, 2017, Accepted December 18, 2017)

Abstract. The prestressed concrete (PSC) technology that was first developed by Freyssinet has significantly improved over the past century in terms of materials and structural design in order to build longer, slender, and more economic structures. The application of prestressing method in structures, which is determined by the pre-tension or post-tension processes, is also affected by the surrounding conditions such as the construction site, workforce skills, and local transportation regulations. This study proposes a prestressed concrete girder design based on a hybrid segment concept. The adopted approach combines both pre-tension and post-tension methods along a simple span bridge girder. The girder was designed using newly developed 2400 MPa PS strands and 60 MPa high-strength concrete. The new concept and high strength materials allowed longer span, lower girder depth, less materials, and slender design without affecting the lateral stability of the girder. In order to validate the applicability of the proposed hybrid prestressed segments girder, a full-scale 35 m girder was fabricated, and experimental tests were performed under various fatigue and static loading conditions. The experimental results confirmed the feasibility of the proposed long-span girder as its performance meets the railway girder standards. In addition, the comparison between the measured load-displacement curve and the simulation results indicate that simulation analysis can predict the behavior of hybrid segments girders.

Keywords: hybrid segment girder, pretension, post-tension, fatigue and static loading test

1. Introduction

Concrete has much lower tensile strength compared to its compressive strength. In order to overcome this limitation, steel reinforcing bars have been used as tensile reinforcement in concrete structures. In addition, prestressing tendons were introduced to improve the performance of concrete as they tend to prestress the concrete structure and control the excessive tensile stress in long span concrete beams (Billington 2004). Recently, prestressed concrete (PSC) has been developed to reduce the depth and increase the span of concrete girders especially in tall buildings or bridge structures. PSC beams can be achieved by either of the following construction processes: pre-tension or post-tension of steel tendons at curing time.

Post-tensioned beams offer much longer span than pre-tensioned beams owing to their minimal deflection properties. On the other hand, pre-tensioned beams are fast and easy to construct which allow the mass production of large quantities of prefabricated PSC components that can be delivered to the construction site in a short time.

However, prestressing requires the transportation and installation of an entire long span component in one piece without intermediate splices and casting at the construction site. New prestressing technologies were proposed (AASHTO LRFD 1998) to address these limitations using new techniques to construct long span structures, such as cable stayed members or extensible cantilever spans. However, these methods involve complicated design and analysis that require skilled labor and high cost to construct. Accordingly, the concrete prestressing method is improved to increase the span by combining both the pre-tensioning and post-tensioning processes.

Post-tensioned beams were fabricated in several pieces per span and subsequently post-tensioned together to obtain long span girders (Seguirant 1998). However, the quality control of post-tension tendons is difficult due to the complexity of the anchorage zone reinforcement. Various scenarios were attempted to combine pre-tensioned and post-tensioned strands for assembling both types of beams (Abdei-Karim and Tadros 1992). Furthermore, Han *et al.* (2003) used both theoretical and experimental observations to examine the performance of multistage prestressing at different loading stages, as this technology was introduced to reduce the depth or increase the span of concrete girders (Han *et al.* 2003). Recently, long-span pre-tensioned prestressed beams were introduced in the US. This technique uses post-tensioning processes to connect the end of girder to the continuous construction of the bridge girder (Aktan and Attanayake 2013). In addition, a double prestress system was developed, using tension from the tendons and compression from the bars, simultaneously

*Corresponding author, Principal Researcher

E-mail: kim.jinkook@posco.com

^aAssistant Professor

E-mail: yimhongjae@gmail.com

^bSenior Researcher

E-mail: jm.yang@posco.com

(Kim *et al.* 2013a). Although these improved PSC methods involve additional construction operations and devices, they allow obtaining longer span and lower depth of the prestressed girders constructed on site.

Rebar assembly and concrete pouring are performed on the construction site and are followed by prestressing after the concrete hardens. Tendons have parabolic profiles to maximize eccentricity at the center while minimizing it at both ends of the span. The number of tendon units, which consist of strands, sheath, and anchorages, is determined by the span length, the web width, and the anchorage zone area. As the span increases, more tendon units are required. This can result in complex reinforcement at the anchorage zone and duct installation areas. The complication at the anchorage zone could worsen quality control and asymmetry of ducts along the span could induce unexpected lateral displacement of beam. Instead, constructing long span post-tensioned beams is achievable because most of the work is carried out at the jobsite. To overcome these limitation, high-strength concrete and PS strand were developed, and the experimental and numerical studies using 2400 MPa PS strand has been reported to investigate its applicability (Kim *et al.* 2016, Yang *et al.* 2016, Kwon *et al.* 2016).

In general, the span of such prestressed railway-bridge girder does not exceed 25 m due to its self-weight limitations. If the span increased, the girder depth can reach 2.8 m and more. Hence, this study proposed a hybrid prestressed segment bridge girder (HPS girder) for a railway-bridge. Total length of proposed HPS girder is 35 m, and there have been no reports on the effect of hybrid concept using high-performance construction materials. The proposed girder is composed of three segments combination with a pre-tensioned mid-segment and post-tension applied to all combined segments. For this purpose, 60 MPa high-strength concrete and 2400 MPa high-strength strands were used. Full-scale HPS girder was fabricated in accordance with the assembling process that proposed based on the predicted prestressing deflection to avoid the risk of manufacturing failure. Fatigue and static loading tests were conducted for the proposed HPS girder including crack width measurements. In addition, displacement by static loading over 2800 kN was compared with the results of simulation analysis, and the feasibility and applicability of the proposed HPS girder was assessed based on the acceptable displacement specifications for railway bridges.

2. The concept of hybrid prestressed segment bridge girder

Design and construction of railway bridge should be considered about dynamic resistance and fatigue loading, and constructed railway bridge is hard to secure a detour when railway bridge has a structural defect. The bridge design should consider the dynamic resistance and fatigue loading. High-speed trains require railway bridges with relatively high load-carrying capacities than highway bridges. The precast PSC I-type girder has been widely used for railway bridges with the bridge decks erected on site. In

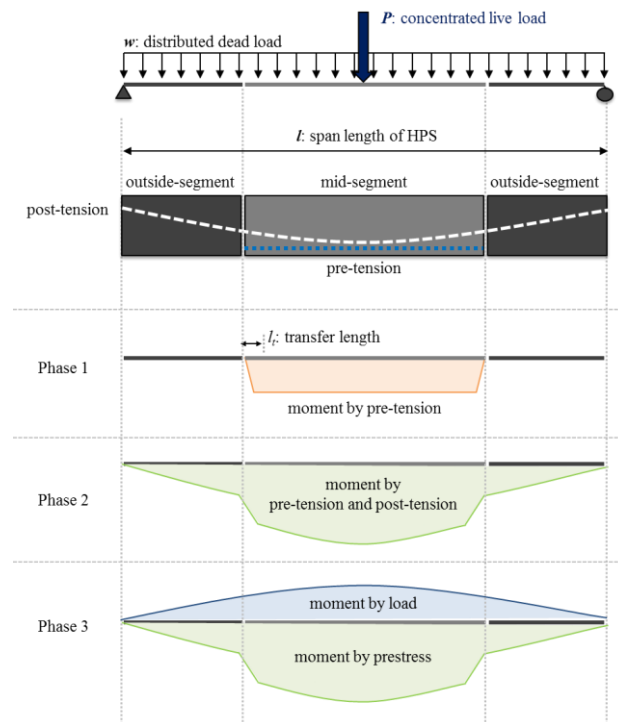


Fig. 1 Schematic of HPS girder segments combination and loading process

precast PSC girders, the forces on PS strands are transferred to the concrete via the bonding force. However, the prestressing force might be reduced after release due to long-term creep or shrinkage of the concrete. The proposed HPS girder has minimum prestressing force loss in the pre-tensioned mid-segment because the hardening and shrinkage have almost been converged before the segments are transferred to the site. Additionally, a long span girder can be achieved with the minimized post-tensioning at the end segments of the girder where prestressing is less required or unnecessary due to the small bending moment. The concept of HPS girders is based on the following assumptions:

- (1) The HPS girder is composed of three segments for a simple beam, where the precast mid-segment is pre-tensioned and all segments are post-tensioned on site.
- (2) The total girder span is 35 m (l), where girder height and web thickness is 2.4 m and 180 mm, respectively.
- (3) The pre-tensioned mid-segment is 15 m long, where PS strand is located on 100 mm from the bottom of segment.
- (4) The other two-outside segments are 10 m long each.
- (5) A uniform distributed dead load (w) acts throughout the length of the girder.
- (6) A concentrated live load (P) is acting on the center of HPS girder.
- (7) The magnitude ratio of dead load and live load is 7:3 ($wl:P=7:3$).

Based on these assumptions, the maximum moment by the dead load is $wl^2/8$ and by the live load is $Pl/4$ at the center of HPS girder. Considering the combination of both external loads, the total moment is calculated as $18.96P$, and the moment at the joints between the outside-segment

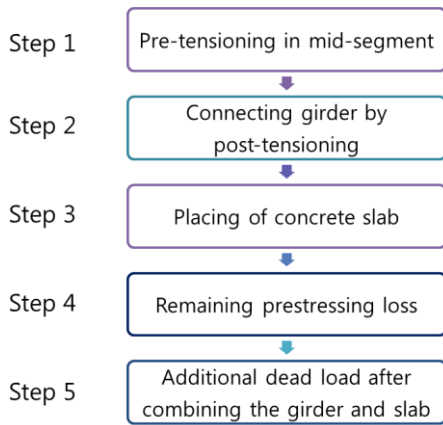


Fig. 2 Flow chart of loading steps for HPS girder

Table 1 Loading steps for prestressing HPS girders

Step	Prestressing force	Sectional properties	Moment by loading
Pre-tensioning in mid-segment	$\frac{P_1(1+R)}{2}$	A_g, Z_g, I_g	M_{d1}
Connecting girder by post-tensioning	$\frac{(P_1 + P_2)(1+R)}{2}$	-	M_{d2}
Placing of concrete slab	-	-	$M_{d2} + M_{d3}$
Additional dead load after combining the girder and slab	-	A_c, Z_c, I_c	$M_{d2} + M_{d3} + M_{d4}$
Remaining prestressing loss	$R(P_1 + P_2)$	-	$M_{d2} + M_{d3} + M_{d4} + M_{(l+i)}$

* P_1 : Pre-tension force

P_2 : Post-tension force

R : Effective ratio of prestress after loss

A_g : Sectional area of girder

Z_g : Section modulus of girder

I_g : Moment of inertia of girder

A_c : Area of composite section of girder and slab

Z_c : Section modulus of composite section

I_c : Moment of inertia of composite section

M_{d1} : Moment by dead load of pre-tensioned segment

M_{d2} : Moment by dead load of full length girder

M_{d3} : Moment by dead load of slab

M_{d4} : Moment by additional dead load

$M_{(l+i)}$: Moment by live load

and mid-segment is $13.33P$. If the pre-tensioned mid-segment can support 30% of total moment ($18.96P$), the amount of post-tension at the outside-segments will be reduced by about 30%. This means that 17% of the post-tension is reduced in the combined HPS girder. In addition, the required internal structures for the PSC girder, such as sheath, anchorage, and anchorage zone reinforcement, are also decreased in HPS girder.

Fig. 1 is a schematic that illustrates the segmental combination and loading process of a HPS girder. It has been reported that a prestress loss of about 50% can be observed during the first four weeks after prestressing. Thus, other assumptions for combining the three segments should be considered including that (1) the section of HPS is uniform along the girder length (2) about 50% pre-tension loss of the mid-segment occurs before post-tensioning (3) about 50% post-tension loss of HPS occurs before the slab combination (4) about 50% of the HPS pre-tension and post-tension occur after the slab combination,

which means that the total prestress loss occurs in three sequential phases during the combining process. Hence, the prestressing force, the sectional properties, and the moment by loading of HPS girder are determined by the five loading steps listed in Table 1. The first step is the pre-tensioning in the mid-segment that involves 50% pre-tension loss. The moment by dead load occurs through the mid-segment, and the prestressing force is determined by the pre-tension force (P_1) and the effective ratio of prestress after loss (R). The second step is connecting the girder by post-tensioning with 50% of post-tension loss. The bending moment by dead load occurs throughout the full length of the girder, and the prestressing force is determined by the pre-tension force and post-tension force (P_2) in addition to the effective ratio of prestress after loss. The third and fourth steps involve placing and combining the slab on the girder. The moment from the additional dead load by the slab occurs, and the sectional properties change to consider the composite section of the girder and slab. The final step involves the remaining prestressing loss $(1+R)(P_1+P_2)/2$. The prestressing force is determined by the total prestress loss, and the moment by live load occurs throughout the full length of the girder.

3. Fabrication of full-scale hybrid prestressed segment bridge girder

In order to experimentally verify the proposed HPS girder, a full-scale PSC I-type beam was fabricated using high strength concrete and 2400 MPa high strength strands. The Railway Design Code (MLIT 2015) was implemented as structural design standard, which is equivalent to AASHTO Standard Specifications for Highway Bridges (AASHTO 2002). The transfer length of 2400 MPa PS strands was based on the results of the study by Yang *et al.* (2016). The concrete was prepared with design compressive strength of 60 MPa for the girder and 27 MPa for the slab. Type 1 Portland cement (specific gravity of 3.15) and fine aggregate river sand (specific gravity of 2.67 in a surface-dry saturated condition) were used. Crushed gravel (specific gravity of 2.71 in a surface-dry saturated condition) was used as the coarse aggregate with a maximum size of 25 mm. About 10% of the mixed binder was replaced by blast furnace slag. In addition, air-entraining admixture was added to the concrete, accounting for about 0.75% of the binder weight. The mix-proportions for concrete girder is described in Table 2.

The recently developed 2400 MPa PS strand used in this experiment has a diameter of 15.2 mm and nominal tensile strength of 2400 MPa or 333 kN. The field application for this newly developed strand was examined by several researchers in the field (Kim *et al.* 2013b, Kim *et al.* 2016, Yang *et al.* 2016). The minimum elongation and maximum relaxation values of the strands were reported as 3.5% and 2.5%, respectively. The obtained load behavior is almost similar to that of the 1860 MPa PS strand excluding the tensile strength, where previous proposed the double prestress system using PS bar and PS tendon of 2400 MPa strength (Kim *et al.* 2013b). Table 3 shows the specific material properties of the used PS strand. Using the 2400

Table 2 Mix proportion of concrete (kg/m³)

Water	Cement	Slag	Fine aggregate	Coarse aggregate	AE admixture
163	559	62	653	909	4.66

Table 3 Material properties of PS strand

Tensile strength (MPa)	Diameter (mm)	Yield load (kN)	Tensile load (kN)	Elongation (%)	Modulus of elasticity (GPa)	Relaxation (%)
2400	15.2	283	333	3.5	185–205	2.5

MPa PS strand can reduce the construction cost because less material will be required for post-tension such as the number of tendons, sheath, and anchorage devices. This can also reduce the girder section and decrease the dead load by self-weights which can allow building long span bridge girders.

The mid and outside segments of the I-girder were fabricated with pre-tension and post-tension forcing. The depth of all segments was 2.4 m. Fig. 3 shows the fabrication procedure of HPS girder that can be described as follows:

(1) The reinforcement (*D13* and *D16*, *SD400*) was placed through the mid-segment.

(2) A total of 6 strands of 2400 MPa were pre-tensioned before the concrete pouring in mid-segment.

(3) Mid-segment concrete was placed and cured for 28 days.

(4) The PS strand was detensioned using cutting and sudden release when the compressive strength of concrete was over 70% of design strength.

(5) Reinforcement and sheath (with a diameter of 110 mm) were placed for the outside-segments.

(6) After placing and curing the outside-segment concrete for 28 days, they were combined with the pre-tensioned mid-segment using epoxy.

(7) 2 post-tensioning tendons (38 strands) were used to prestress the combined segments.

(8) The upper slab was reinforced and placed.

The cross-section of the fabricated segments was 1000 mm × 2400 mm, and the total girder length was 35 m. The pre-tensioned strands were placed at a height of 100 mm on the mid-segment. The post-tensioned strands had a parabolic drape and were arranged uniformly. The dimensions and geometrical specifications of the tested HPS girder are shown in Fig. 4 and Table 4. Han *et al.* (2003) proposed prestressed concrete girder with multistage prestressing concept. This study compared with the multistage prestressing girder that constructed in site. The compared results are described in Table 4. The geometric aspects of the HPS girder are improved owing to the use of advanced construction materials. The high-strength concrete (60 MPa) and PS strands (2400 MPa) were effectively used, thus the girder depth was decreased by about 200 mm. As only two tendons were used for post-tensioning, the web thickness of the combined segments was decreased by about 20 mm. The results obtained by the proposed prestressed girders compared to the multistage prestressing girder are presented in Table 4. The design conditions for reinforced concrete slab are also described in Table 5. The displacement of mid-segment was measured during the

Table 4 Design conditions of the tested HPS girder compared with 35 m long girder with multistage prestressing concept

	HPS	Multistage prestressing girder
Compressive strength of concrete girder	60 MPa	40 MPa
Concrete stressing at prestressing	48 MPa	32 MPa
Tensile Strength of PS strand	2400 MPa	1860 MPa
Number of tendons and sheath for post-tension	2	6
Tendon units	Pretension : 6 strands Post-tension : 19 Hx2 sets	1 st post-tension : 12 Hx4 sets 2 nd post-tension : 6 Hx2 sets
Total weight of PS	1800 kg	2530 kg
Yield strength of rebar	400 MPa	400 MPa
Length of mid-span	15 m	-
Length of outside-span	10 m	-
Total length of girder	35 m	35 m
Girder height	2.4 m	2.6 m
Web thickness	180 mm	200 mm
Diameter of sheath	110 mm	80 mm (1 st) / 75 mm (2 nd)

Table 5 Design conditions for reinforced concrete slab

Compressive strength of concrete slab	27 MPa
Yield strength of rebar	400 MPa
Slab height	280 mm
Slab length	35 m

detensioning of the 6 strands. It was reported that the displacement at the center of mid-segment after release is 0.68 mm in the vertical direction and 0.3 mm in the horizontal direction. Meanwhile, the final displacement at the center of combined girder after post-tensioning is 43.53 mm in vertical direction and 17.05 mm in horizontal direction. The unexpected lateral displacement may be attributed to fabrication errors at the connections of segments, and theoretical lateral displacement should be zero. However, the reported lateral displacement is much lower than the standard requirement for precast beams (BS EN 1992), which is 0.3% of the girder length (105 mm for a 35 m long girder). The symmetrical arrangement of tendons along the entire girder length should minimize the unexpected lateral displacement despite its reduced depth and slender cross section.

4. Loading test of hybrid prestressed segment bridge girder

Fatigue loading and static loading tests were performed using the full-scale HPS girder described above. A force control test protocol of up to 817 kN was performed using two million bending cyclic loads with frequency of 0.6 Hz applied at the center of mid-segment to evaluate the fatigue performance and stiffness of the tested HPS girder. The applied load followed the service load standards of the railway design code (MLIT 2015). No visual cracks were observed during the cyclic loading test, not even around the segments joints. Fig. 5 illustrates the plotted hysteresis

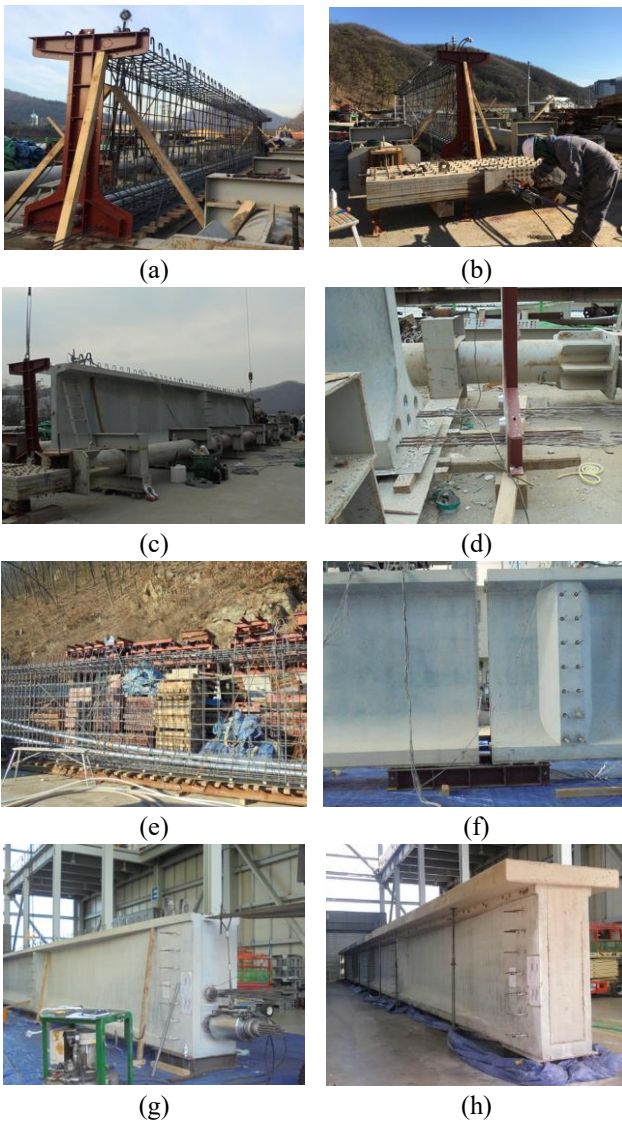


Fig. 3 Fabrication procedure of HPS: (a) reinforcement placed for mid-segment; (b) pre-tension of PS strands before concrete placing; (c) concrete placing and curing of mid-segment; (d) detensioning of mid-segment via sudden release; (e) placing the reinforcement and sheath for outside-segment; (f) combining pretensioned mid-segment and cured outside-segments using epoxy; (g) post-tension through all segments; (h) placing of concrete slab with reinforcement

curves of the measured load-displacement. As shown in Fig. 5, the load-displacement curve is horizontally shifted within 14 mm range of the increased displacement; however, the slope of load-displacement curve corresponds to the increase of cyclic loading. The shifted curve seems to be due to the movement at the support point of the girder or caused by the stabilizing of the heterogeneous concrete material. The identical slope can also indicate that the stiffness of HPS girder has been maintained without critical damage during service loading.

Next, a three-point flexural loading method was used to perform the static loading test of HPS girder under the simple support condition. The loading force was increased

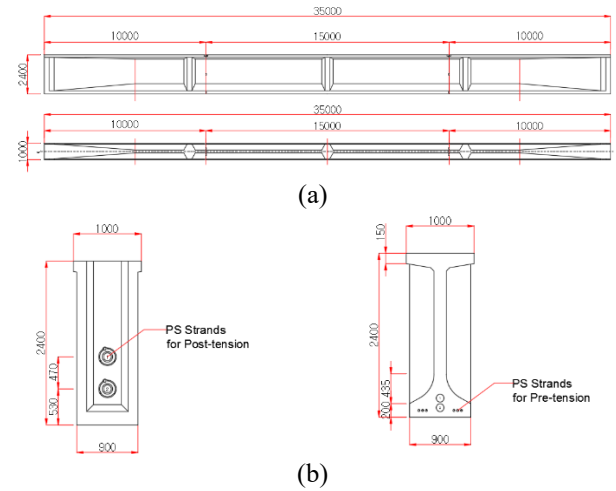


Fig. 4 Geometry of HPS girder (unit: mm): (a) front view and top view and (b) cross-section at the end and center of girder

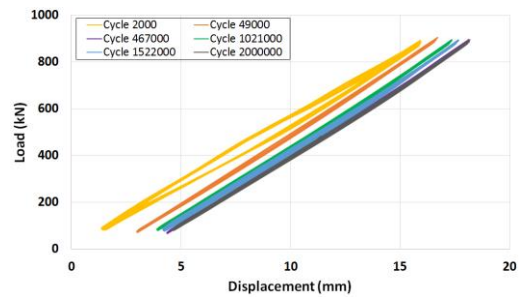


Fig. 5 Load-displacement hysteresis curve of fatigue loading at the center of HPS girder



Fig. 6 Experimental loading test and measurement of displacement at the center of girder

up to 2830 kN under quasi-static load. The displacement in the vertical direction was measured during the test at the

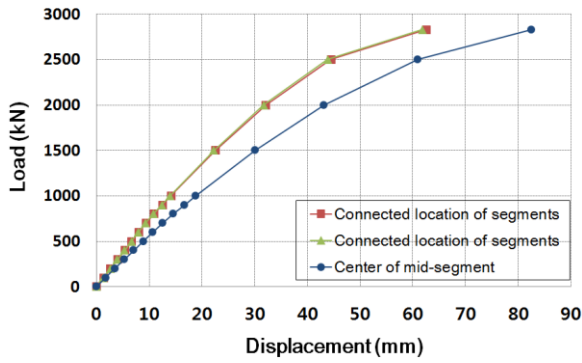


Fig. 7 Load-displacement curve by static loading test of HPS girder

Table 6 Measured crack width of HPS girder reported during the loading test

Load (kN)	Crack width (mm)
0	0.00
500	0.02
1000	0.04
1500	0.06
2000	0.09
2500	0.13
2830	0.19

center of girder and at the joints between mid-segment and outside-segments. The displacement transducer (CDP-50, Tokyo Sokki Kenkyujo) was used for these measurements, as shown in Fig. 6. The obtained load-displacement curves were plotted in Fig. 7. An initial cracking was observed at center of girder when the loading force was increased to approximately 2000 kN. From that point on, the crack propagation was monitored using a crack measurement sensor (PI-5-50, Tokyo Sokki Kenkyujo) for the loading forces of 2000 kN, 2300 kN, 2500 kN, and 2830 kN. The crack width was measured at different loading forces up to the maximum load of 2830 kN, as listed in Table 6. The obtained crack patterns are also illustrated in Fig. 8. These results indicate that despite the different materials and structural system, the performance of the tested hybrid segment bridge girder with 2400 MPa PS strands is similar to the conventional cast-in-place 1860 MPa monolithic post-tensioned prestressed concrete girder.

5. Verification based on the simulation result

A numerical analysis was conducted to verify that the hybrid prestressing of both pre-tension and post-tension at a section of 2400 MPa PS strand are compatible with the results obtained from the numerical analysis method. This was based on the sectional analysis using MATLAB at the mid-span under the assumption of strain compatibility and force equilibrium in the section. The result was extended to the full-length girder based on the assumed parabolic deformation curve. In order to consider the sequential fabrication, the pretensioned mid segment was separately

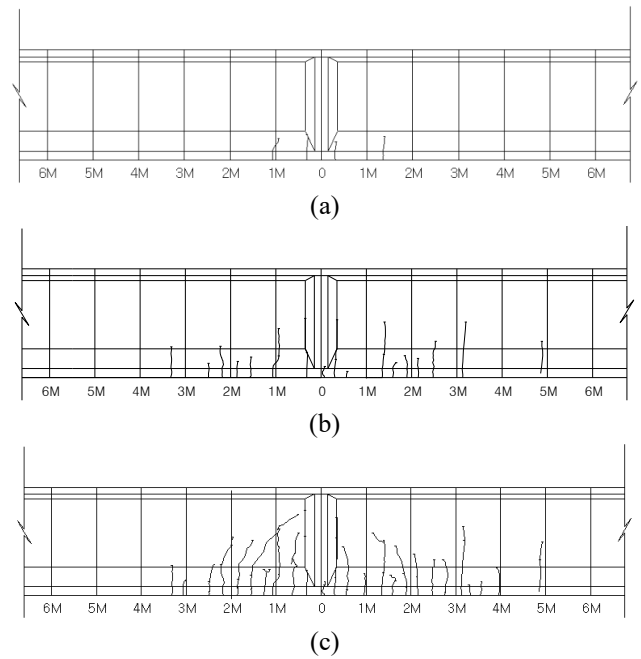


Fig. 8 Crack patterns of HPS girder when static loading of (a) 2000 kN, (b) 2300 kN, and (c) 2500 kN were applied

calculated and the results was applied as the initial condition for numerical analysis. Several more assumptions were taken such as: (1) tensile resistance of concrete is zero; (2) failure of the girder happens when any one of strains at concrete or tendon reaches their ultimate strains; (3) the cross-section along the span length is uniform because the effect of enlarged post-tensioning anchorage zone at both ends could be negligible in the overall flexural behavior of girder. Popovics's concrete stress-strain model, which is appropriate for high strengths over 50 MPa and Ramberg-Osgood's model for high strength PS strand were used (Park *et al.* 2012, Park *et al.* 2017) for the numerical calculation. Fig. 9 compares the reported experimental results and the results obtained by the simulation analysis. It was found that the load-displacement curve obtained from static test of HPS girder was well matched with the numerical simulation results considering the cumulated stress in construction step.

The vertical displacement obtained under the maximum loading state of 2830 kN by experimental loading test and simulation analysis at the center of the HPS girder were 82.57 mm and 82.68 mm, respectively. However, the vertical displacement obtained under cracking loading state of 2000 kN by the experimental loading test and simulation analysis were 43.22 mm and 37.22 mm, respectively. Although both the obtained displacement values are slightly different at the cracking loading state, the load-displacement curves are almost similar throughout the static loading test. This result proves that the simulation analysis can predict the behavior of HPS girder under various loading conditions. The specifications provided by the American Railway Engineering and Maintenance-of-Way Association indicate that the deflection of prestressed flexural members of bridge structures shall be designed within $l/640$ of the span under the service live load

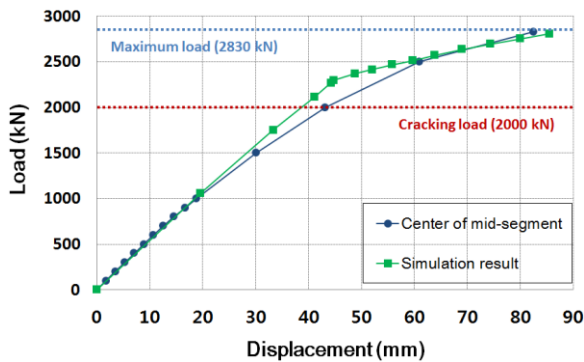


Fig. 9 Compared load-displacement curves of static loading test and simulation results at the center of HPS girder

(AREMA 2007). Based on this specification, the displacement allowed for a 35 m long girder is 54.69 mm. According to the plotted load-displacement hysteresis curve of fatigue loading, the maximum measured displacement of about 18 mm obtained at center of HPS girder satisfies the railway specification. Furthermore, the load-displacement curve of HPS girder shows a displacement of 54.69 mm at the static loading of about 2300 kN. This means that proposed HPS girder fully meets the deflection standards to be used as railway structure under various loading conditions.

The proposed HPS girders are subject to dynamic deformation that induced by the moving loads on railway bridges. Accordingly, a dynamic analysis based on an experimental approach is required to verify the dynamic performance of the proposed girders including the damping ratio, natural frequency, and vibration. The focus of future research should be on analyzing the dynamic behavior including long-term behavior by friction loss or anchorage loss based on the currently obtained experimental and simulated results.

6. Conclusions

This study proposed a hybrid prestressed segment girder using 60 MPa high-strength concrete and 2400 MPa PS strand. A full-scale HPS girder was fabricated using a combined pre-tension and post-tension method. Experimental tests were performed under various loading conditions. In addition, the result of simulation analysis was compared with the obtained experimental results of the static loading tests. Based on the study findings, the following conclusions were drawn:

- The hybrid segments system using high-strength PS strand of 2400 MPa allows the construction of longer and slender bridge girders using less material.
- Fewer inserted tendons, less complex reinforcement, and reduced internal structures will be needed to fabricate the proposed HPS girder than those required for the conventional PSC girders.
- According to the experimental loading test results, the HPS girders can highly control the occurrence of crack under lateral stability.
- The measured load-displacement hysteresis curve

under the fatigue loading condition indicates that the performance of HPS girder meets the service loading standards for railway bridges.

- Based on the railway specification, the HPS girder can satisfy the deflection limitation standards up to 2300 kN of static loading.
- The simulation analysis can predict the behavior of HPS girder under various loading conditions.

Acknowledgments

This research was supported by a grant (13SCIPA01) from Smart Civil Infrastructure Research Program funded by Ministry of Land, Infrastructure and Transport(MOLIT) of Korea government and Korea Agency for Infrastructure Technology Advancement(KAIA), and This work was supported by the National Research Foundation of Korea (NRF) grant funded by the Korea government (MSIP) (No. 2015R1C1A1A01055474).

References

- AASHTO, L.R.F.D. (1998), *Bridge Design Specifications*.
- Abdei-Karim, A.M. and Tadros, M.K. (1992), *State-of-the-Art of Precast/Prestressed Concrete Spliced-/Girder Bridges*, Precast/Prestressed Concrete Institute, Chicago, Illinois, U.S.A.
- Aktan, H. and Attanayake, U. (2013), *Improving Bridges with Prefabricated Precast Concrete Systems*, (No. RC-1602).
- American Association of State Highway, and Transportation Officials (2002), *Standard Specifications for Highway Bridges*, AASHTO.
- AREMA, L.M.D. (2013), *American Railway Engineering and Maintenance-of-Way Association*, Manual for Railway Engineering.
- Billington, D.P. (2004), "Historical perspective on prestressed concrete", *PCI J.*, **49**(1), 14-30.
- British Standards Institution (2004), *Eurocode 2: Design of Concrete Structures: Part 1-1: General Rules and Rules for Buildings*, British Standards Institution.
- Han, M.Y., Hwang, E.S. and Lee, C. (2003), "Prestressed concrete girder with multistage prestressing concept", *Struct. J.*, **100**(6), 723-731.
- Kim, J.K., Yang, J.M. and Yim, H.J. (2016), "Evaluation of transfer length in pretensioned prestressed concrete beam using 2,400 MPa PS strand", *J. Struct. Eng.*, **142**(11), 04016088.
- Kim^a, J.K., Seong, T.R., Jang, K.P. and Kwon, S.H. (2013), "Tensile behavior of new 2,200 MPa and 2,400 MPa strands according to various types of mono anchorage", *Struct. Eng. Mech.*, **47**(3), 383-399.
- Kim^b, C.E., Kim, J.K. and Kim, J.K. (2013), "Behaviour of double prestress system in prestressed concrete girders", *Mag. Concrete Res.*, **65**(14), 855-864.
- Kwon, S.H., Jo, S.D., Lee, S.G. and Kim, C.Y. (2016), "Ductility enhancement of 60-m long span prestressed concrete girder using new high strength prestressed strands (2,160 and 2,400 MPa)", *J. Struct. Integr. Mainten.*, **1**(2), 73-80.
- Ministry of Land, Infrastructure and Transportation (MLIT), Korea Rail Network Authority (KR) (2015), *Railway Design Code*, Ministry of Land, Infrastructure and Transportation.
- Park, H. and Cho, J.Y. (2017), "Ductility analysis of prestressed concrete members with high-strength strands and code implications", *ACI Struct. J.*, **114**(2), 407-416.
- Park, H., Cho, J.Y. and Kim, J.S. (2017), "Investigation on

- applicability of 2400 MPa strand for posttensioned prestressed concrete girders”, *KCI J.*, **24**(6), 727-735.
- Seguirant, S.J. (1998), “New deep WSDOT standard sections extend spans of prestressed concrete girders”, *PCI J.*, **43**(4), 92-119.
- Yang, J.M., Yim, H.J. and Kim, J.K. (2016), “Transfer length of 2400 MPa seven-wire 15.2 mm steel strands in high-strength pretensioned prestressed concrete beam”, *Smart Struct. Syst.*, **17**(4), 577-591.

CC